

Special Section on Transporters in Drug Disposition and Pharmacokinetic Prediction

Interindividual Differences in the Expression of ATP-Binding Cassette and Solute Carrier Family Transporters in Human Skin: DNA Methylation Regulates Transcriptional Activity of the Human *ABCC3* Gene[□]

Tomoki Takechi, Takeshi Hirota, Tatsuya Sakai, Natsumi Maeda, Daisuke Kobayashi, and Ichiro Ieiri

Department of Clinical Pharmacokinetics, Graduate School of Pharmaceutical Sciences, Kyushu University, Fukuoka, Japan (T.T., T.H., T.S., N.M., I.I.); Drug Development Research Laboratories, Kyoto R&D Center, Maruho Co., Ltd., Kyoto, Japan (T.T.); and Department of Clinical Pharmacy and Pharmaceutical Care, Graduate School of Pharmaceutical Sciences, Kyushu University, Fukuoka, Japan (D.K.)

Received October 19, 2017; accepted January 30, 2018

ABSTRACT

The identification of drug transporters expressed in human skin and interindividual differences in gene expression is important for understanding the role of drug transporters in human skin. In the present study, we evaluated the expression of ATP-binding cassette (ABC) and solute carrier (SLC) transporters using human skin tissues. In skin samples, *ABCC3* was expressed at the highest levels, followed by *SLCO3A1*, *SLC22A3*, *SLC16A7*, *ABCA2*, *ABCC1*, and *SLCO2B1*. Among the quantitated transporters, *ABCC3* accounted for 20.0% of the total mean transporter mRNA content. The expression of *ABCC3* mRNA showed large interindividual variability (9.5-fold). None of the single nucleotide polymorphisms tested (-1767G>A, -1328G>A, -1213C>G, -897delC, -260T>A, and -211C>T) in the promoter region of the *ABCC3* gene showed a significant change in *ABCC3* mRNA

levels. *ABCC3* expression levels negatively correlated with the methylation status of the CpG island (CGI) located approximately 10 kilobase pairs upstream of *ABCC3* ($R_s = -0.323, P < 0.05$). The reporter gene assay revealed a significant increase in transcriptional activity in the presence of CGI. *ABCC3* mRNA was upregulated in HaCaT cells by the demethylating agent 5-aza-2'-deoxycytidine. Furthermore, the deletion of the region surrounding CGI using the clustered regularly interspaced short palindromic repeat/Cas9 system resulted in significantly lower *ABCC3* mRNA levels than those in control clones in HaCaT cells. Herein, we demonstrated large interindividual differences in the expression of drug transporters in human skin. CGI may function as an enhancer of the transcription of *ABCC3*, and methylation levels in CGI contribute to the variability of *ABCC3* expression in human skin.

Introduction

Membrane transporters have broad specificity and facilitate the uptake and efflux of their substrates across plasma membranes. Two major superfamilies, the ATP-binding cassette (ABC) and solute carrier (SLC) families, strongly influence the absorption, distribution, and excretion of drugs. Previous studies suggested that transporters play a role in *in vivo* drug pharmacokinetics, and transporter-mediated drug-drug interactions were recently identified (Schneck et al., 2004; Shitara et al., 2004; Neuvonen et al., 2006; Klatt et al., 2011). The accumulation of evidence has revealed that variabilities in the expression and

activities of some transporters affect pharmacokinetics as well as pharmacological and/or toxicological effects (Cascorbi, 2006; Ieiri et al., 2006; Maeda and Sugiyama, 2008; Gotanda et al., 2015).

Genetic polymorphisms are one of the most important factors influencing variable gene expression. Single nucleotide polymorphisms (SNPs) in pharmacokinetic-related genes play a critical role in interindividual variations in pharmacokinetics and drug responses (Ieiri et al., 2009; Ma and Lu, 2011). In addition to genetic polymorphisms, epigenetic mechanisms, including DNA methylation in clusters of CpG dinucleotides, called CpG islands (CGIs), also contribute to the variability of gene expression (Yasar et al., 2013). Previous studies indicated that DNA methylation plays an important role in the interindividual variability in drug transporter gene expression (Saito et al., 2011; Wu et al., 2015).

Skin is the largest organ in the human body. It consists of multiple layers (the stratum corneum, epidermis, dermis, and subcutaneous tissue) and acts

This work was supported by the Japan Research Foundation for Clinical Pharmacology.

<https://doi.org/10.1124/dmd.117.079061>

□ This article has supplemental material available at dmd.aspetjournals.org.

ABBREVIATIONS: ABC, ATP-binding cassette; 5-aza-dC, 5-aza-2'-deoxycytidine; bp, base pair; CG, cytosine-guanine; CGI, CpG island; COBRA, combined bisulfate restriction analysis; CRISPR, clustered regularly interspaced short palindromic repeat; GAPDH, glyceraldehyde 3-phosphate dehydrogenase; kbp, kilobase pair; MRP, multidrug resistance-associated protein; NHEK, normal human epidermal keratinocyte; PCR, polymerase chain reaction; sgRNA, single guide RNA; SLC, solute carrier; SNP, single nucleotide polymorphism; TIS, translation initiation site.

as both a physical and chemical permeability barrier. The stratum corneum, the most superficial layer of the epidermis, is considered to be the major diffusion barrier that limits the transdermal penetration of xenobiotics. Notwithstanding this barrier function, a growing number of strategies (Lane, 2013; Ita, 2016) have been developed to deliver drugs to and through skin, because transdermal delivery has a number of advantages, such as avoidance of the first-pass effect of the liver and minimization of pain, over the oral, hypodermic, and intravenous routes (Prausnitz and Langer, 2008). Although the skin penetration of xenobiotics was previously attributed to passive diffusion, increasing evidence indicates that transporters have a function in the biochemical barrier of skin epithelial cells beneath the stratum corneum. For example, the constitutive expression of multidrug resistance proteins (MRPs) has been detected in normal human epidermal keratinocytes (NHEKs), which are the predominant cells in the epidermis (Baron et al., 2001). Furthermore, previous studies showed that NHEKs exhibit functional transporter-mediated uptake and efflux activity (Schiffer et al., 2003; Heise et al., 2010). A recent transport study demonstrated that ABC transporters in different compartments of the skin contribute to the transdermal absorption of a typical substrate in mice (Hashimoto et al., 2013). These findings suggest that transporters play an important role in the disposition of drugs, at least in murine skin and human keratinocyte cell cultures. However, it is important to note that previous studies using cell cultures, animal models, or only a small number of skin tissues were mostly inadequate for quantitative analyses of transporter expression in human skin. Large interindividual variabilities in the expression of transporters may lead to inappropriate drug concentrations, causing drug toxicity or insufficient therapeutic effects in skin. Therefore, interindividual variability in the expression levels of transporters needs to be identified by evaluating expression levels in a large number of skin tissues.

The aims of the present study were to assess the expression levels of ABC and SLC transporters in human skin and elucidate the mechanisms responsible for variability in mRNA expression. The transporters analyzed (26 ABC and 25 SLC transporters) were selected based on their relevance as drug transporters (International Transporter Consortium, 2010; European Medicines Agency, 2012; FDA Center for Drug Evaluation and Research, 2012; Roth et al., 2012) and previous studies showing transporter expression in human skin (Baron et al., 2001; Schiffer et al., 2003; Kielar et al., 2003; Markó et al., 2012). We examined genetic variations in the promoter regions of *ABCC3*, which showed large interindividual variability in expression levels in this study. We performed a DNA methylation analysis to clarify the relationship between the methylation status and mRNA levels in human skin. The contribution of CGI to *ABCC3* expression was examined using the luciferase reporter assay and a deletion analysis of CGI in HaCaT cells using the clustered regularly interspaced short palindromic repeat (CRISPR)/Cas9 system.

Materials and Methods

Skin Tissues. Human full-thickness skin tissues from 48 Caucasian females were purchased from Biopredic International (Saint Grégoire, France). The skin tissues were derived from healthy adults. The average (\pm S.D.) age of the skin tissue donors was 45.9 ± 10.8 years, with a range of 22–64 years. Anatomic sites were abdomen ($n = 33$) and breast ($n = 15$). The donor information is summarized in Supplemental Table 1. All tissue specimens were obtained with informed consent, and this study was approved by the Ethics Committee at Kyushu University.

Cell Culture. A HaCaT human keratinocyte line was obtained from Cell Lines Service (Heidelberg, Germany). HaCaT cells were grown in Dulbecco's modified Eagle's medium (Sigma-Aldrich, St. Louis, MO) supplemented with 10% fetal bovine serum (Nichirei Biosciences Inc., Tokyo, Japan) and incubated at 37°C in a 5% CO₂ atmosphere. The culture medium was replaced every 2 or 3 days. Cells were routinely passaged before reaching confluence.

Isolation of Total RNA from Human Skin and cDNA Synthesis. Total RNA was isolated from each tissue using an RNeasy Fibrous Tissue Mini Kit (Qiagen, Hilden, Germany). RNA samples were reverse-transcribed into first-strand

cDNA with approximately 300–2000 ng of total RNA, $1 \times$ first-strand buffer, 20 mM dithiothreitol, 0.5 μ g of random primer (Promega, Madison, WI), 2 mM deoxynucleotide mixture, and 200 U of SuperScript II RNase H⁻ reverse transcriptase (Life Technologies, Carlsbad, CA). The reaction was run at 42°C for 60 minutes. Reverse-transcription reactions were always performed in the presence or absence of reverse transcriptase to ensure that genomic DNA did not contaminate subsequent polymerase chain reaction (PCR). cDNA was stored at -30°C until used.

Quantitative Real-Time PCR. mRNA levels were measured by real-time PCR using an ABI PRISM 7000 sequence detection system (Applied Biosystems, Foster City, CA). The sequences of the primers used in this study are summarized in Supplemental Table 2. Amplification mixtures contained 5 μ l of SYBR Premix Ex Taq (Takara, Kyoto, Japan), 0.2 μ l of Rox reference dye, 2 μ l of a cDNA synthesis mixture, 2 pmol each of the forward and reverse primers, and distilled water in a total volume of 10 μ l. Cycling conditions were as follows: 30 seconds at 95°C, followed by 40 cycles of amplification at 95°C for 5 seconds and at 60°C for 30 seconds. The specificity of the real-time PCR product was proven by a dissociation curve analysis. Triplicate measurements were performed for all samples. To compare gene expression levels among different samples, the amount of target mRNA was corrected relative to that of glyceraldehyde 3-phosphate dehydrogenase (GAPDH). GAPDH has been used as an internal reference in gene expression analysis using human skin (Takenaka et al., 2013; Fujiwara et al., 2014), and the expression of GAPDH showed a small interindividual variation in human skin (Osman-Ponchet et al., 2014). Real-time PCR data for each target gene quantity were calculated in the following two ways.

In the Pfaffl method, the ratio of target gene to GAPDH gene was evaluated as follows:

$$\text{ratio} = E_{\text{target}}^{\Delta C_t \text{ target}(\text{reference} - \text{test})} / E_{\text{GAPDH}}^{\Delta C_t \text{ GAPDH}(\text{reference} - \text{test})}$$

where E_{target} = amplification efficiency of the target gene, E_{GAPDH} = amplification efficiency of the GAPDH gene, $\Delta C_t \text{ target}$ = the difference between C_t of the target gene in the reference sample and test sample, and $\Delta C_t \text{ GAPDH}$ = the difference between C_t of the GAPDH gene in the reference sample and test sample.

With absolute quantification, each 96-well assay plate contained unknown samples and sequentially diluted concentrations of the plasmid standard constructed, from which a standard curve was generated for the quantification of gene copy numbers in unknown samples.

Genotyping and Haplotype Analysis. Genomic DNA was isolated from skin specimens with a NucleoSpin Tissue kit (Macherey-Nagel, Düren, Germany) according to the manufacturer's protocol. Six SNPs ($-1767\text{G}>\text{A}$, $-1328\text{G}>\text{A}$, $-1213\text{C}>\text{G}$, -897delC , $-260\text{T}>\text{A}$, and $-211\text{C}>\text{T}$) in the promoter region of *ABCC3* (Lang et al., 2004; Sasaki et al., 2011) were genotyped in 48 skin donors by a PCR-restriction fragment length polymorphism analysis and direct sequencing. The sequences of primers are given in Supplemental Table 3. PCR was performed using approximately 10 ng of genomic DNA with 250 nM each primer and AmpliTaq Gold DNA polymerase (Life Technologies) in a total volume of 10 μ l. The following amplification conditions were used: an initial denaturation step of 95°C for 9 minutes followed by 40 cycles of denaturation at 95°C for 40 seconds, annealing at 55.7 or 62.3°C for 45 seconds, extension at 72°C for 40 seconds, and a final extension at 72°C for 5 minutes. Regarding $-1767\text{G}>\text{A}$, PCR products were digested by *Bsm*I and then electrophoresed on a 3% agarose gel. Direct sequencing using an ABI 3100 automatic sequencer (Applied Biosystems) with a Big-Dye Terminator Cycle Sequencing Ready Reaction Kit (Applied Biosystems) was applied to all other SNPs. The sequence was inspected for deviations from the original *ABCC3* (GenBank accession no. NC_000017.11), which was defined as the reference. Haplotypes of the promoter region were estimated with ARLEQUIN version 3.5 software (Excoffier L et al., 2010). A linkage disequilibrium analysis was performed with Haploview (Broad Institute, Cambridge, MA).

Bisulfite Conversion and Combined Bisulfite Restriction Analysis. CGIs located within 20 kilobase pairs (kbp) up- and downstream of *ABCC3* were identified by the CpG Island Searcher Program (Takai and Jones, 2003). CGIs were defined using the following criteria: guanine-cytosine > 50%, observed CpG/expected CpG > 0.60, length > 200 base pairs (bp), and the gap between an adjacent island > 100 bp. Bisulfite conversion and subsequent purification were performed using the EpiTect Bisulfite Kit (Qiagen) according to the manufacturer's protocol. Bisulfite-converted genomic DNA was subjected to PCR using bisulfite conversion-specific primers. PCR was performed by initial denaturation at 95°C for 9 minutes, followed by 40–45 cycles of 95°C for 40 seconds, 50–65°C

for 45 seconds, 72°C for 40 seconds, and finally by extension at 72°C for 5 minutes. PCR products were digested with each restriction enzyme based on a methylation-dependent restriction site. Primers for the combined bisulfate restriction analysis (COBRA) and restriction enzymes are provided in Supplemental Table 4. The digested PCR products were electrophoresed on 3% agarose gels and visualized by ethidium bromide staining. The intensity of bands was quantified with LAS-3000 (Fujifilm, Tokyo, Japan). The proportion of methylated versus unmethylated DNA was assessed from the relative intensity of cut and uncut PCR products. Episcopo-methylated HCT116 gDNA and unmethylated HCT116 DKO gDNA (Takara) were used as the positive methylation and unmethylation controls, respectively.

Reporter Gene Vector Constructs. In the functional analysis of *ABCC3* CGI-6, three reporter gene vectors were constructed: pGL4.10-CGI, including CGI-6 ranging from -9954 to -9635 bp relative to translation initiation site (TIS); pGL4.10-Pro, including the promoter ranging from -2013 to -1 bp relative to TIS; and pGL4.10-CGI/Pro, including CGI-6 and the promoter. The oligonucleotide sequences used for PCR are listed in Supplemental Table 5. The insert sequences of all resulting constructs were verified by direct sequencing.

Cell Transfection and Reporter Gene Assays. In reporter gene assays, 48.2 fmol of each vector construct with 25 ng of pRL-TK (Promega) as an internal control was transfected into HaCaT cells using Lipofectamine 3000 reagent (Life Technologies). Cells were harvested 48 hours after transfection, and firefly and renilla luciferase were both assayed using the Dual-Luciferase system reporter assay (Promega). Relative reporter gene activities were calculated by dividing the firefly luciferase activity of the reporter construct by the renilla luciferase activity of pRL-TK. Transfection was performed in triplicate, and at least three independent experiments were conducted.

Demethylation Experiments in HaCaT Cells. HaCaT cells were treated with 3 μ M 5-aza-2'-deoxycytidine (5-aza-dC; Sigma-Aldrich) and 0.1% dimethylsulfoxide as a vehicle control for 72 hours. Total RNA was isolated from cells, and *ABCC3* mRNA expression levels were measured using quantitative real-time PCR.

Deletion of CGI Using the CRISPR/Cas9 System. The pGL3-U6-sgRNA-PGK-puromycin vector (ID: 51133; Addgene, Cambridge, MA) and Guide-it CRISPR/Cas9 System Kit (Takara) were used to generate vectors encoding a single guide RNA (sgRNA) and puromycin resistance or sgRNA and Cas9, respectively. Guide RNAs targeting the CGI locus were designed using CRISPR-Redirect (<http://crispr.dbcls.jp/>). DNA oligonucleotides harboring 20 variable nucleotide sequences for Cas9 targeting were annealed to generate short double-strand DNA fragments with 4-bp overhangs compatible with ligation into the *BsaI* site of the pGL3-U6-sgRNA-PGK-puromycin vector or pGuide-it CRISPR/Cas9 vector. To create an HaCaT cell line that deletes CGI-6, HaCaT cells were seeded on a six-well plate at a density of 4.0×10^5 cells/well and transfected using Lipofectamine 3000 (Life Technologies) with 2.5 μ g of each vector. To select transfected cells, 1 μ g/ml puromycin was added to the cell growth medium for 2 days. Cells were cloned by limiting dilutions, and DNA was extracted from the

cloned cells for PCR amplification. PCR products were characterized by electrophoresis and sequencing to analyze the region deleted by the CRISPR/Cas9 system. *ABCC3* mRNA expression in three deleted clones and four control clones was evaluated using a quantitative real-time PCR. The sequences of oligos and primers are described in Supplemental Table 6.

Statistical Analysis. Statistical analyses were conducted with R (version 3.0.0; A Language and Environment for Statistical Computing, Vienna, Austria) and S plus (Mathematical Systems, Inc., Tokyo, Japan). The Mann-Whitney *U* test or Kruskal-Wallis rank sum test was applied to gene expression data stratified according to genotype. Spearman's rank-order correlation analysis was used to test for correlations between the DNA methylation status and gene expression. In other cases, differences between groups were analyzed using Student's *t* test when only two groups were present. Differences were considered to be significant when *P* values were less than 0.05.

Results

Gene Expression of ABC and SLC Transporters in Human Skin.

Sixteen out of the 51 transporter genes were present at the levels quantitated ($C_t < 31$), 21 were at the levels detected ($31 \leq C_t \leq 35$), and 14 were below the detection limit ($35 < C_t$; Table 1). Based on the results of the first screening, we selected transporters with a mean C_t value < 31 for absolute quantification. *ABCB1* and *ABCG2* transporters, which are transporters that are expressed in human skin, were added to the analysis. Quantification revealed that expression of the *ABCC3* gene coding for the MRP3 transporter was the most abundant, followed by *SLCO3A1*, *SLC22A3*, *SLC16A7*, *ABCA2*, *ABCC1*, and *SLCO2B1* (Fig. 1A). Among the quantitated transporters, *ABCC3* accounted for 20.0% of the total mean transporter mRNA content, whereas the top three transporters accounted for approximately half of the expression levels in human skin (Fig. 1B). These results also indicated that the expression of *ABCB1*, *ABCA7*, and *ABCG2* was very weak. Among the top three transporters in the quantification, interindividual variations ($n = 48$) in mRNA levels in *ABCC3* and *SLC22A3* were markedly greater (9.5- and 14.2-fold differences, respectively) than that in *SLCO3A1* (4.2-fold). Typical substrates of the top three transporters are summarized in Supplemental Table 7.

ABCC3 Genetic Variants, Allele Frequencies, and Haplotypes.

Six SNPs in the promoter region of *ABCC3* were genotyped in 48 skin samples of Caucasian female origin. Allele frequencies were 9.4%, 2.1%, 7.3%, 32.3%, 7.3%, and 60.4% for -1767G>A (rs1989983), -1328G>A (rs72837520), -1213C>G (rs62059725), -897delC (rs35467079), -260T>A (rs9895420), and -211C>T (rs4793665), respectively (Table 2). Seven haplotypes were identified with a

TABLE 1

First-step screening for the evaluation of transporter expression in Caucasian skin samples

In easy comparisons (first screening), the mean cycle threshold (C_t) value of each transporter was calculated. One-sixteenth of pooled cDNA was used as a template for real-time PCR. Pooled cDNA was prepared by mixing an identical volume of cDNA ($n = 20$). C_t values > 35 , in the range of 31–35, and < 31 were interpreted as the absence of gene expression, the presence of gene expression but below the limit of quantitation, and the presence of gene expression at the quantitative level, respectively.

Gene	C_t Mean	Gene	C_t Mean	Gene	C_t Mean	Gene	C_t Mean
<i>ABCA1</i>	28.9	<i>ABCC2</i>	33.4	<i>SLC15A1</i>	30.6	<i>SLC22A8</i>	>35
<i>ABCA2</i>	29.1	<i>ABCC3</i>	27.0	<i>SLC15A2</i>	32.5	<i>SLC22A10</i>	>35
<i>ABCA3</i>	31.1	<i>ABCC4</i>	32.2	<i>SLC16A1</i>	29.7	<i>SLC22A11</i>	>35
<i>ABCA4</i>	>35	<i>ABCC5</i>	28.4	<i>SLC16A3</i>	33.3	<i>SLC46A1</i>	32.5
<i>ABCA5</i>	29.0	<i>ABCC6</i>	32.2	<i>SLC16A7</i>	30.0	<i>SLC47A1</i>	29.2
<i>ABCA6</i>	32.3	<i>ABCC8</i>	>35	<i>SLC16A8</i>	>35	<i>SLC47A2</i>	30.4
<i>ABCA7</i>	30.7	<i>ABCC10</i>	33.2	<i>SLC22A1</i>	32.9	<i>SLCO1A2</i>	>35
<i>ABCA8</i>	31.2	<i>ABCC11</i>	33.6	<i>SLC22A2</i>	>35	<i>SLCO1B1</i>	>35
<i>ABCA9</i>	32.1	<i>ABCC12</i>	>35	<i>SLC22A3</i>	28.6	<i>SLCO1B3</i>	>35
<i>ABCA10</i>	31.2	<i>ABCG1</i>	29.9	<i>SLC22A4</i>	33.0	<i>SLCO2B1</i>	30.1
<i>ABCA12</i>	31.8	<i>ABCG2</i>	32.9	<i>SLC22A5</i>	30.2	<i>SLCO3A1</i>	28.9
<i>ABCB1</i>	32.1	<i>ABCG5</i>	34.4	<i>SLC22A6</i>	>35	<i>SLCO4A1</i>	33.7
<i>ABCC1</i>	29.3	<i>ABCG8</i>	>35	<i>SLC22A7</i>	>35		

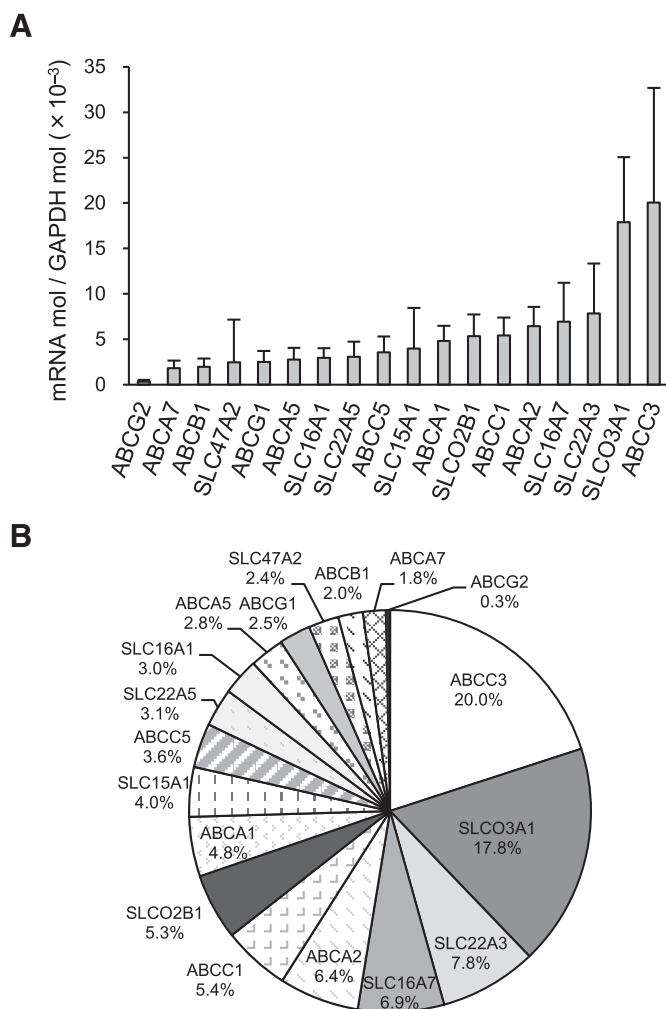


Fig. 1. Quantification of ABC and SLC transporter mRNAs in Caucasian skin samples. (A) Absolute transporter mRNA levels were evaluated in human skin samples ($n = 18$). Regarding absolute quantification, each 96-well assay plate contained unknown samples and sequentially diluted concentrations of the plasmid standard constructed, from which a standard curve was generated for the quantification of gene copy numbers in unknown samples. To compare gene expression levels among different samples, the amount of target mRNA was corrected to that of GAPDH. (B) The mean mRNA expression level of each transporter is expressed as a percentage of the total mean transporter mRNA content.

frequency ranging between 0.74% and 32.3% (Table 3). The linkage disequilibrium between each of the three SNPs (rs1989983, rs62059725,

and rs9895420) was high ($r^2 = 0.76-1.0$), and rs62059725 and rs9895420 showed complete linkage. No deviations from the Hardy-Weinberg equilibrium were observed ($P > 0.05$).

Relationship between Genetic Variants and ABCC3 Expression Levels. No significant differences were observed in expression levels among samples with haplotype pattern 5, 6, or 7 (data not shown). None of the other SNPs were associated with changes in expression levels (data not shown).

Analysis of the DNA Methylation Status among Different Skin Samples by COBRA. After extensive examinations of 20 kbp up- and downstream of *ABCC3*, nine CGIs were identified (Table 4). Among the 16 selected CG (cytosine-guanine) sites within CGIs, three (-308 , -35 , and $+163$ bp relative to TIS) were predominantly unmethylated, whereas another three ($-16,169$, $+9877$, and $+20,266$ bp relative to TIS) were heavily methylated. There was moderate to high methylation variability between skin samples, ranging between 4- and 153-fold in the remaining 10 CG sites (Fig. 2A).

Relationship between ABCC3 mRNA Expression and DNA Methylation Levels. To analyze the relationship between *ABCC3* expression and DNA methylation levels, we performed Spearman's regression analysis on real-time PCR and COBRA data from the 48 skin samples studied. As shown in Fig. 2B, the DNA methylation levels of the CG site (-9718 loci relative to TIS) in CGI-6 negatively correlated with *ABCC3* mRNA expression in skin samples. No other CGIs showed a negative correlation between *ABCC3* mRNA expression and DNA methylation levels (data not shown).

Effects of CGI-6 on Transcriptional Activity of the ABCC3 Promoter. To functionally evaluate CGI-6, we used different reporter gene constructs containing *ABCC3* promoter fragments and/or CGI-6 for reporter gene assays (Fig. 3). The results obtained indicated that CGI-6 exhibits no promoter activity. In contrast, luciferase activity was significantly higher in cells transfected with pGL4.10-CGI/Pro than in other cell cultures transfected with pGL4.10-Pro. These results indicate that CGI-6 exhibits regulatory activity and plays a role as an enhancer.

Increased ABCC3 Expression Induced by the 5-aza-dC Treatment. To evaluate the effects of DNA methylation on *ABCC3* expression, we treated the HaCaT cell line with the DNA methyltransferase inhibitor 5-aza-dC (Fig. 4). The CGI-6 methylation status and *ABCC3* mRNA expression levels were assessed by COBRA and real-time PCR. Treatment with 5-aza-dC led to a weaker methylation status in CGI-6 than in the control group (data not shown). A corresponding increase in *ABCC3* mRNA was observed in cells exposed to the demethylating agent.

Decreased ABCC3 Expression Induced by CGI-6 Disruption Using the CRISPR/Cas9 System. To investigate the contribution of

TABLE 2
ABCC3 genetic variations in Caucasian skin samples

Position ^a	Reference Allele ^b	Variant Allele	Genotype			Frequency of Variant Allele	HW P Val	NCBI SNP ID
			R/R	R/V	V/V			
						%		
-1767	agagGcatc	agagAcatc	39	9	0	9.4	1.0000	rs1989983
-1328	gcttGcccc	gcttAcccc	46	2	0	2.1	1.0000	rs72837520
-1213	tggaCagac	tggaGagac	41	7	0	7.3	1.0000	rs62059725
-897	ccttCcccc	cctt-cccc	24	17	7	32.3	0.2858	rs35467079
-260	ttgcTtggc	ttgcAtggc	41	7	0	7.3	1.0000	rs9895420
-211	ccccCacct	ccccTacct	10	18	20	60.4	0.2026	rs4793665

HW P val, Hardy-Weinberg P value; ID, identifier; NCBI, National Center for Biotechnology Information; R, reference allele; V, variant allele.

^aWith respect to the TIS of the *ABCC3* gene; A in ATG is designated as +1 and that immediately following the 5' base is designated as -1.

^bGenBank accession no. NC_000017.11.

TABLE 3
Estimated haplotypes in *ABCC3* gene in Caucasian skin samples

Nucleotides that are different from the reference sequence are underlined>.

Haplotype	-1767G>A	-1328G>A	-1213C>G	-897delC	-260T>A	-211C>T	Frequency
#1	<u>A</u>	<u>A</u>	<u>G</u>	C	<u>A</u>	C	%
#2	<u>A</u>	<u>G</u>	<u>C</u>	C	<u>T</u>	C	0.74
#3	<u>A</u>	G	<u>G</u>	C	<u>A</u>	C	2.08
#4	<u>G</u>	<u>A</u>	<u>C</u>	C	<u>T</u>	C	6.56
#5	G	<u>G</u>	C	C	T	C	1.35
#6	G	G	C	C	T	<u>T</u>	28.9
#7	G	G	C	<u>Del</u>	T	<u>T</u>	28.1
							32.3

Del, deletion of the nucleotide.

CGI-6 to *ABCC3* mRNA expression, we disrupted the region surrounding CGI-6 in HaCaT cells using the CRISPR/Cas9 system. We confirmed targeted disruption by PCR amplification (Fig. 5, A and B) and direct sequencing (data not shown). Quantitative real-time PCR showed significantly weaker *ABCC3* mRNA expression in disrupted clones than in control clones (Fig. 5C).

Discussion

An increasing number of studies have recognized drug transporters as an important factor in pharmacokinetics as well as pharmacological and/or toxicological effects (Cascorbi 2006; Maeda and Sugiyama, 2008; Ieiri et al., 2009). Recent studies suggested that drug transporters play a role in the disposition of drugs in murine skin and human keratinocyte cell cultures (Schiffer et al., 2003; Heise et al., 2010; Hashimoto et al., 2013). These findings prompted speculation that interindividual variability in the expression of drug transporters may lead to inappropriate drug levels and associated toxicity or inefficacy in skin. Thus, the identification of expressed drug transporters and their variability in human skin is important for elucidating the role of drug transporters in human skin. In the present study, we demonstrated large interindividual differences in the expression of drug transporters in human skin. We also showed that DNA methylation in CGI located approximately 10 kbp upstream of *ABCC3* regulated its expression levels in normal human skin.

Twenty-two ABC and 15 SLC transporters were expressed at detectable levels in human skin, and *ABCC3*, *SLCO3A1*, *SLC22A3*, *SLC16A7*, *ABCA2*, *ABCC1*, and *SLCO2B1* were strongly expressed in skin. In previous studies, expression comparisons among drug transporters in human skin tissues were limited to the findings of relative quantification (Li et al., 2006; Takenaka et al., 2013; Fujiwara et al., 2014).

TABLE 4
Location of CGIs in the region surrounding *ABCC3*

Name	Start ^a	End ^a	%GC	Obs/Exp	Length
CGI-1	-20,090	-19,881	53.3	0.603	210
CGI-2	-16,357	-16,153	56.6	0.600	205
CGI-3	-15,643	-15,423	50.7	0.608	221
CGI-4	-13,873	-13,600	60.6	0.604	274
CGI-5	-13,448	-13,221	57.5	0.603	228
CGI-6	-9874	-9674	57.7	0.600	201
CGI-7	-429	502	70.7	0.732	931
CGI-8	9717	10,205	54.4	0.611	489
CGI-9	19,852	20,429	53.6	0.657	578

Exp, expected CpG; %GC, guanine-cytosine content in CGI; Obs, observed CpG.
^aWith respect to the TIS of the *ABCC3* gene.

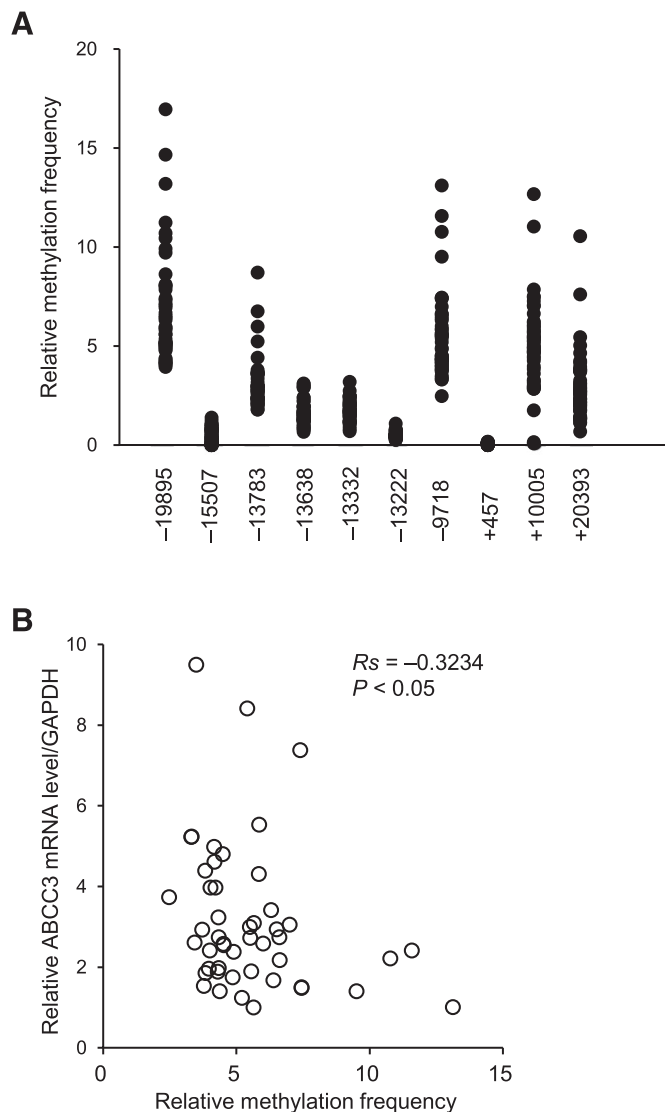


Fig. 2. Correlation analysis between *ABCC3* mRNA levels and methylation frequencies of CGI in Caucasian skin samples. (A) DNA methylation differences in CGIs surrounding the *ABCC3* gene. Relative methylation frequencies were assessed by COBRA using human skin samples ($n = 48$). The y-axis represents the band intensity ratio of the methylated status to unmethylated status. The x-axis represents the CG locus relative to TIS. (B) Negative correlation between *ABCC3* mRNA expression and methylation levels at the CG site (-9718 loci relative to TIS) in CGI-6 ($n = 48$). R_s and P values are from Spearman's rank-order correlation analysis.

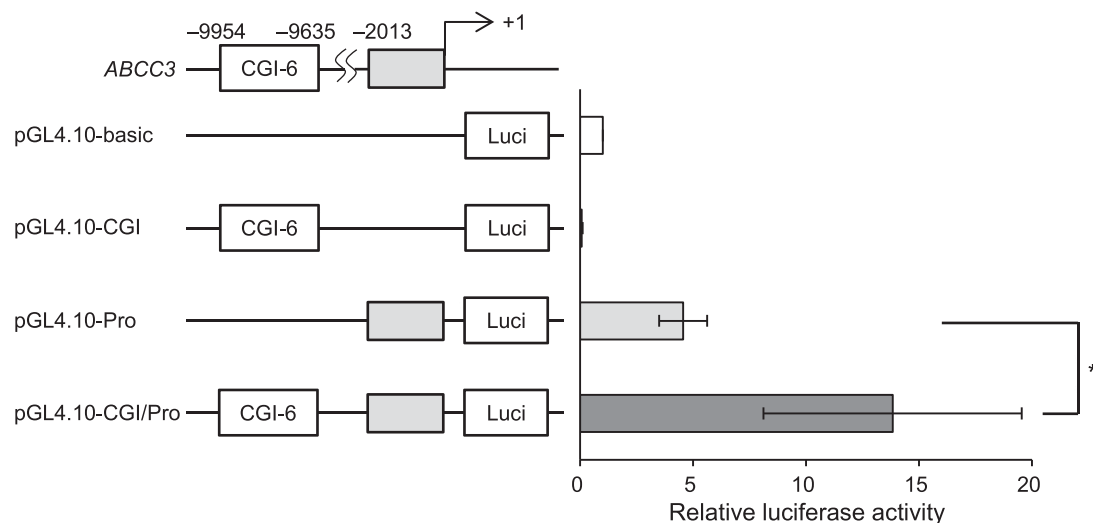


Fig. 3. Effects of CGI-6 on luciferase activities. Luciferase (Luci) reporter gene constructs were transiently transfected into HaCaT cells. Luciferase values were normalized to the pRL-TK vector. Data represent the mean \pm S.D. ($n = 4$) and mean value obtained with the pGL4.10-basic vector as 100%. * $P < 0.05$, statistically analyzed using Student's t test.

This study was the first to absolutely quantify the expression of drug transporters in human skin using a large number of skin tissues. It is important to note that the isoforms of expressed drug transporters in human skin were consistent with previous findings (Kielar et al., 2003; Li et al., 2006; Markó et al., 2012; Takenaka et al., 2013; Fujiwara et al., 2014). Previous studies showed constitutive expression of ABCC3 in NHEK by immunoblots and the functional ABCC-mediated efflux activity of NHEK using in vitro transport assay (Baron et al., 2001; Heise et al., 2010). Skin consists of heterogeneous cell populations, such as keratinocytes and fibroblasts. Therefore, to evaluate the function of ABCC3, it is important to identify which cells and layers express ABCC3 in future studies.

Next, we focused on the mechanisms responsible for the variability in ABCC3 expression, which was the strongest in human skin, assuming that high mRNA levels are more relevant for transporter function. The variant analysis of the *ABCC3* gene showed that genetic polymorphisms in the promoter region of *ABCC3* did not correlate with the interindividual variability in ABCC3 expression in human skin. This is not in agreement with previous studies showing that $-211C>T$ significantly decreased ABCC3 mRNA levels in the human liver (Lang et al., 2004; Sasaki et al., 2011). One possible explanation for this discrepancy is transcription factors binding to the region including the $-211T$ allele, which is expressed in the human liver but not in skin. On the other hand, our results are consistent with an in vivo analysis showing that $-211C>T$ had no influence on ABCC3 expression levels in patients with acute leukemia (Doerfel et al., 2006). Further studies using human skin are required to clarify whether promoter variants contribute to ABCC3 expression in human skin. In addition to genetic polymorphisms, we analyzed the correlation between ABCC3 expression and age. A previous study suggested an age-associated decrease in the function of transporters (Toomvliet et al., 2006). In our study, the significant association was not observed (Supplemental Fig. 1).

The epigenetic regulation of gene expression plays an important role in the interindividual variability in the gene expression of drug transporters (Saito et al., 2011; Wu et al., 2015). We attempted to identify the underlying epigenetic mechanisms for interindividual variability in ABCC3 mRNA expression in human skin. Our results showed that ABCC3 mRNA expression levels negatively correlated with the methylation levels of the CG site (-9718) in CGI-6 located

approximately 10 kbp upstream of the *ABCC3* gene. Previous studies reported that DNA methylation in gene promoters plays an important role in gene transcription (Schaeffeler et al., 2011; Ikehata et al., 2012). However, our results revealed that methylation levels in CGIs surrounding the promoter of *ABCC3* did not affect ABCC3 mRNA expression. To investigate the role of CGI-6 methylation in ABCC3 expression, we analyzed the methylation status of CGI-6 and ABCC3 mRNA levels in cells treated with or without a 5-aza-dC demethylating agent. The demethylation treatment of HaCaT cells led to about 2-fold reduction in the degree of methylation in CGI-6 (data not shown) and about 1.7-fold increase in ABCC3 mRNA levels. Previous studies reported that methylation of the *ABCC3* promoter region was not involved in ABCC3 mRNA levels in some cancer cell lines (Worm et al., 2001; Zolk et al., 2013). These findings suggest that the methylation of CGI-6 plays a role in regulating ABCC3 mRNA expression in HaCaT cells.

CGIs are often located around or in more distant regions of gene promoters, and their function is to regulate transcription (Illingworth and Bird, 2009; Deaton and Bird, 2011). The results of the luciferase reporter assay showed that CGI-6 did not exhibit promoter activity, but displayed enhancer activity. Furthermore, in HaCaT cells, the disruption of the region surrounding CGI-6 led to significantly decreased ABCC3 mRNA levels. COBRA analysis revealed that CGI-6 was not hypermethylated (about 50%) in HaCaT cells (data not shown), thus the disruption of CGI-6 caused reduced ABCC3 expression. These results suggest that CGI-6 regulates the transcriptional activity of *ABCC3*, and are consistent with previous findings showing that CGIs distant from the target gene locus affected gene expression (Yoon et al., 2002, 2005), whereas enhancers located far from gene promoters regulated transcription (Hilton et al., 2015; Ferreira et al., 2016). Our results are also supported by previous findings showing that the methylation of enhancers affects gene expression (Hoivik et al., 2011; Yang et al., 2012). Few studies have examined the molecular mechanisms of transcriptional regulation of ABCC3. Luciferase assay with a series of truncated 5'-flanking regions indicated that the region from -127 to -23 bp is important for ABCC3 expression (Takada et al., 2000). In addition, it was demonstrated that ABCC3 is under the control of TATA-less promoter, and Sp1 binding sites may be involved in the transcription. Another study reported that nuclear receptor retinoic X receptor- α -retinoic acid receptor- α (RXR α :RAR α) functions as a repressor of MRP3 activation

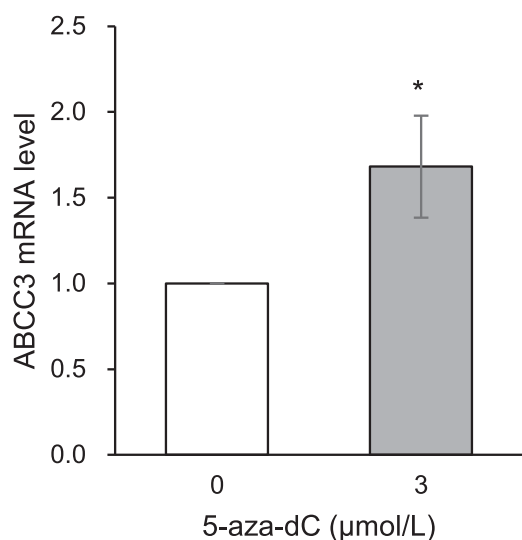


Fig. 4. Effects of 5-aza-dC on ABCC3 mRNA expression in HaCaT cells. HaCaT cells were treated with 3 $\mu\text{mol/l}$ 5-aza-dC for 72 hours. ABCC3 mRNA expression levels were assessed using real-time PCR and normalized to the expression of GAPDH. Data represent the mean \pm S.D. of triplicate experiments. * $P < 0.05$, statistically analyzed using Student's t test.

by reducing Sp1 binding to -113 to -108 bp with respect to the *ABCC3* TIS (Chen et al., 2007). However, few studies have reported the relationship between ABCC3 expression and DNA methylation.

The CG site (-9718) showed the association with ABCC3 mRNA expression. The methylation levels in the CG site (-9718) was not positively associated with the other CG site (Supplemental Fig. 2). This result suggests that the CGI-6 including the CG site (-9718) plays a key role in the interindividual difference of ABCC3 expression in human skin. As a result of an in silico search for transcriptional factors binding to CGI-6 (P-Match 1.0 Public, <http://gene-regulation.com/pub/programs.html#pmatch>), zinc finger protein was predicted. It has been reported that a family of human zinc finger proteins bind to methylated DNA and repress transcription (Filion et al., 2006). Since a negative correlation was found between the DNA methylation status of CGI-6 and ABCC3 expression levels in human skin, the binding amount of zinc finger protein to CGI-6 may be changed depending on the DNA methylation status of CGI-6, and subsequently, the transcription of ABCC3 may be regulated.

It was reported that interindividual differences in ABCC3 protein expression in lung cancer strongly correlate with ABCC3 mRNA expression (Young et al., 1999, 2001). Our study did not evaluate the protein expression in human skin. The importance of interindividual differences in ABCC3 mRNA expression in human skin will be clarified by additional studies: correlation of mRNA levels with protein levels and drug transport in human skin.

In summary, we conducted a profile analysis of 26 ABC and 25 SLC transporter isoforms using a large number of skin tissues and showed that ABCC3 was expressed at the highest levels. The present study is the first to characterize the drug transporters expressed in human skin as absolute quantitative values. Our results showed that large interindividual differences exist in the expression of drug transporters in human skin, and methylation levels in CGI contribute to the variability of ABCC3 expression in skin.

The role of transporters is not well known in human skin. ABCC1, which is part of the ABCC family, is expressed in keratinocytes. Interestingly, it was suggested that ABCC1 contributes to the transdermal absorption of substrate drug in human skin

(Osman-Ponchet et al., 2014). Similar results were also reported for ABCB1 and ABCG2 (Skazik et al., 2011; Hashimoto et al., 2013). These reports suggest that the ABC family in human skin has an important role in the transdermal absorption of their substrates, but the role of ABCC3 is not clear. The evaluation of the ABCC3 transport activities of the substrates is important to identify the contribution of transdermal absorption in further studies. To date, no clinically relevant drug-drug interactions involving ABCC3 have been reported. ABCC3 transports a wide range of substrates, such as endogenous substances (leukotriene C4, estradiol-17 β -glucuronide), anticancer drugs (methotrexate, etoposide), and other drugs (acetaminophen glucuronide and fexofenadine) (Supplemental Table 7). Therefore, ABCC3 may be responsible for unexpected substance-induced reactions in skin. Our results will contribute to future studies on the disposition of endogenous and exogenous substances and may be very beneficial to the development of personalized medicine.

Acknowledgments

The authors appreciate the technical assistance provided by The Research Support Center, Research Center for Human Disease Modeling, Kyushu University Graduate School of Medical Sciences.

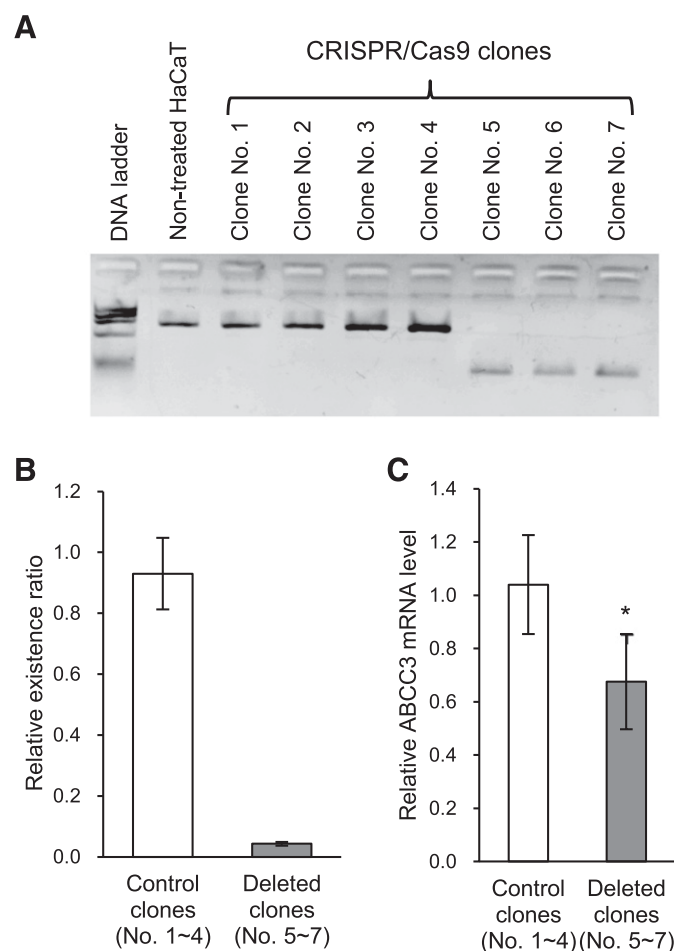


Fig. 5. Effects of the deletion of CGI-6 on ABCC3 mRNA expression in HaCaT cells. (A) Electrophoresis of PCR products spanning the deleted region locus. (B) Quantification of CGI-6 by real-time PCR using primers located on the inside of the deleted region. Data represent the mean \pm S.D., and results were normalized to the region of the *ACTB* gene. (C) Each ABCC3 mRNA level in the established clones was assessed by real-time PCR. Data represent the mean \pm S.D. (four control clones and three deleted clones), and results were normalized to GAPDH mRNA levels. * $P < 0.05$, statistically analyzed using Student's t test.

Authorship Contributions

Participated in research design: Takechi, Hirota, Ieiri.

Conducted experiments: Takechi, Hirota, Sakai, Maeda.

Performed data analyses: Takechi, Hirota, Sakai, Maeda.

Wrote or contributed to the writing of the manuscript: Takechi, Hirota, Kobayashi, Ieiri.

References

- Baron JM, Höller D, Schiffer R, Frankenberg S, Neis M, Merk HF, and Jugert FK (2001) Expression of multiple cytochrome p450 enzymes and multidrug resistance-associated transport proteins in human skin keratinocytes. *J Invest Dermatol* **116**:541–548.
- Cascorbi I (2006) Role of pharmacogenetics of ATP-binding cassette transporters in the pharmacokinetics of drugs. *Pharmacol Ther* **112**:457–473.
- Chen W, Cai SY, Xu S, Denson LA, Soroka CJ, and Boyer JL (2007) Nuclear receptors RXR α : RAR α are repressors for human MRP3 expression. *Am J Physiol Gastrointest Liver Physiol* **292**:G1221–G1227.
- Deaton AM and Bird A (2011) CpG islands and the regulation of transcription. *Genes Dev* **25**:1010–1022.
- Doerfel C, Rump A, Sauerbrey A, Gruhn B, Zintl F, and Steinbach D (2006) In acute leukemia, the polymorphism -211C>T in the promoter region of the multidrug resistance-associated protein 3 (MRP3) does not determine the expression level of the gene. *Pharmacogenet Genomics* **16**:149–150.
- European Medicines Agency (2012) Guideline on the investigation of drug interactions, European Medicines Agency, London.
- Excoffier L and Lischer HE (2010) Arlequin suite ver 3.5: a new series of programs to perform population genetics analyses under Linux and Windows. *Mol Ecol Resour* **10**:564–567.
- FDA Center for Drug Evaluation and Research (2012) Guidance for industry: drug interaction studies – study design, data analysis, implications for dosing, and labeling recommendations, Food and Drug Administration, Washington, DC.
- Ferreira LM, Meissner TB, Mikkelsen TS, Mallard W, O'Donnell CW, Tilburgs T, Gomes HA, Camahort R, Sherwood RI, Gifford DK, et al. (2016) A distant trophoblast-specific enhancer controls HLA-G expression at the maternal-fetal interface. *Proc Natl Acad Sci USA* **113**:5364–5369.
- Filion GJ, Zhenilo S, Salozhin S, Yamada D, Prokhorchouk E, and Defossez PA (2006) A family of human zinc finger proteins that bind methylated DNA and repress transcription. *Mol Cell Biol* **26**:169–181.
- Fujiwara R, Takenaka S, Hashimoto M, Narawa T, and Itoh T (2014) Expression of human solute carrier family transporters in skin: possible contributor to drug-induced skin disorders. *Sci Rep* **4**:5251.
- Gotanda K, Tokumoto T, Hirota T, Fukae M, and Ieiri I (2015) Sulfasalazine disposition in a subject with 376C>T (nonsense mutation) and 421C>A variants in the ABCG2 gene. *Br J Clin Pharmacol* **80**:1236–1237.
- Hashimoto N, Nakamichi N, Uwafuji S, Yoshida K, Sugiura T, Tsuji A, and Kato Y (2013) ATP binding cassette transporters in two distinct compartments of the skin contribute to dermal absorption of a typical substrate. *J Control Release* **165**:54–61.
- Heise R, Skazik C, Rodriguez F, Stanzel S, Marquardt Y, Jousen S, Wendel AF, Wosnitza M, Merk HF, and Baron JM (2010) Active transport of contact allergens and steroid hormones in epidermal keratinocytes is mediated by multidrug resistance related proteins. *J Invest Dermatol* **130**:305–308.
- Hilton IB, D'Ippolito AM, Vockley CM, Thakore PI, Crawford GE, Reddy TE, and Gersbach CA (2015) Epigenome editing by a CRISPR-Cas9-based acetyltransferase activates genes from promoters and enhancers. *Nat Biotechnol* **33**:510–517.
- Hoivik EA, Bjanesoy TE, Mai O, Okamoto S, Minokoshi Y, Shima Y, Morohashi K, Boehm U, and Bakke M (2011) DNA methylation of intronic enhancers directs tissue-specific expression of steroidogenic factor 1/adrenal 4 binding protein (SF-1/Ad4BP). *Endocrinology* **152**:2100–2112.
- Ieiri I, Higuchi S, and Sugiyama Y (2009) Genetic polymorphisms of uptake (OATP1B1, 1B3) and efflux (MRP2, BCRP) transporters: implications for inter-individual differences in the pharmacokinetics and pharmacodynamics of statins and other clinically relevant drugs. *Expert Opin Drug Metab Toxicol* **5**:703–729.
- Ieiri I, Takane H, Hirota T, Otsubo K, and Higuchi S (2006) Genetic polymorphisms of drug transporters: pharmacokinetic and pharmacodynamic consequences in pharmacotherapy. *Expert Opin Drug Metab Toxicol* **2**:651–674.
- Ikehata M, Ueda K, and Iwakawa S (2012) Different involvement of DNA methylation and histone deacetylation in the expression of solute-carrier transporters in 4 colon cancer cell lines. *Biol Pharm Bull* **35**:301–307.
- Illingworth RS and Bird AP (2009) CpG islands—'a rough guide'. *FEBS Lett* **583**:1713–1720.
- Ita K (2016) Perspectives on transdermal electroporation. *Pharmaceutics* **8**.
- Kielar D, Kaminski WE, Liebisch G, Piehler A, Wenzel JJ, Möhle C, Heimerl S, Langmann T, Friedrich SO, Böttcher A, et al. (2003) Adenosine triphosphate binding cassette (ABC) transporters are expressed and regulated during terminal keratinocyte differentiation: a potential role for ABCA7 in epidermal lipid reorganization. *J Invest Dermatol* **121**:465–474.
- Klatt S, Fromm MF, and König J (2011) Transporter-mediated drug-drug interactions with oral antidiabetic drugs. *Pharmaceutics* **3**:680–705.
- Lane ME (2013) Skin penetration enhancers. *Int J Pharm* **447**:12–21.
- Lang T, Hitzl M, Burk O, Mornhinweg E, Keil A, Kerb R, Klein K, Zanger UM, Eichelbaum M, and Fromm MF (2004) Genetic polymorphisms in the multidrug resistance-associated protein 3 (ABCC3, MRP3) gene and relationship to its mRNA and protein expression in human liver. *Pharmacogenetics* **14**:155–164.
- Li Q, Tsuji H, Kato Y, Sai Y, Kubo Y, and Tsuji A (2006) Characterization of the transdermal transport of flurbiprofen and indomethacin. *J Control Release* **110**:542–556.
- Ma Q and Lu AY (2011) Pharmacogenetics, pharmacogenomics, and individualized medicine. *Pharmacol Rev* **63**:437–459.
- Maeda K and Sugiyama Y (2008) Impact of genetic polymorphisms of transporters on the pharmacokinetic, pharmacodynamic and toxicological properties of anionic drugs. *Drug Metab Pharmacokinet* **23**:223–235.
- Markó L, Paragh G, Ungocsi P, Boettcher A, Vogt T, Schling P, Balogh A, Tarabin V, Orsó E, Wikonkál N, et al. (2012) Keratinocyte ATP binding cassette transporter expression is regulated by ultraviolet light. *J Photochem Photobiol B* **116**:79–88.
- Neuvonen PJ, Niemi M, and Backman JT (2006) Drug interactions with lipid-lowering drugs: mechanisms and clinical relevance. *Clin Pharmacol Ther* **80**:565–581.
- Osman-Ponchet H, Boulai A, Koudih M, Sevin K, Alriquet M, Gaborit A, Bertino B, Comby P, and Ruty B (2014) Characterization of ABC transporters in human skin. *Drug Metabol Drug Interact* **29**:91–100.
- Prausnitz MR and Langer R (2008) Transdermal drug delivery. *Nat Biotechnol* **26**:1261–1268.
- Roth M, Obaidat A, and Hagenbuch B (2012) OATPs, OATs and OCTs: the organic anion and cation transporters of the SLCO and SLC22A gene superfamilies. *Br J Pharmacol* **165**:1260–1287.
- Saito J, Hirota T, Kikunaga N, Otsubo K, and Ieiri I (2011) Interindividual differences in placental expression of the SLC22A2 (OCT2) gene: relationship to epigenetic variations in the 5'-upstream regulatory region. *J Pharm Sci* **100**:3875–3883.
- Sasaki T, Hirota T, Ryokai Y, Kobayashi D, Kimura M, Irie S, Higuchi S, and Ieiri I (2011) Systematic screening of human ABCC3 polymorphisms and their effects on MRP3 expression and function. *Drug Metab Pharmacokinet* **26**:374–386.
- Schaeffeler E, Hellerbrand C, Nies AT, Winter S, Kruck S, Hofmann U, van der Kuip H, Zanger UM, Koepsell H, and Schwab M (2011) DNA methylation is associated with downregulation of the organic cation transporter OCT1 (SLC22A1) in human hepatocellular carcinoma. *Genome Med* **3**:82.
- Schiffer R, Neis M, Höller D, Rodríguez F, Geier A, Gartung C, Lammert F, Dreuw A, Zwadlo-Klarwasser G, Merk H, et al. (2003) Active influx transport is mediated by members of the organic anion transporting polypeptide family in human epidermal keratinocytes. *J Invest Dermatol* **120**:285–291.
- Schneck DW, Birmingham BK, Zalikowski JA, Mitchell PD, Wang Y, Martin PD, Lasseter KC, Brown CD, Windass AS, and Raza A (2004) The effect of gemfibrozil on the pharmacokinetics of rosuvastatin. *Clin Pharmacol Ther* **75**:455–463.
- Shitara Y, Hirano M, Sato H, and Sugiyama Y (2004) Gemfibrozil and its glucuronide inhibit the organic anion transporting polypeptide 2 (OATP2/OATP1B1:SLC21A6)-mediated hepatic uptake and CYP2C8-mediated metabolism of cerivastatin: analysis of the mechanism of the clinically relevant drug-drug interaction between cerivastatin and gemfibrozil. *J Pharmacol Exp Ther* **311**:228–236.
- Skazik C, Wenzel J, Marquardt Y, Kim A, Merk HF, Bickers DR, and Baron JM (2011) P-glycoprotein (ABCB1) expression in human skin is mainly restricted to dermal components. *Exp Dermatol* **20**:450–452.
- Takada T, Suzuki H, and Sugiyama Y (2000) Characterization of 5'-flanking region of human MRP3. *Biochem Biophys Res Commun* **270**:728–732.
- Takai D and Jones PA (2003) The CpG island searcher: a new WWW resource. *In Silico Biol* **3**:235–240.
- Takenaka S, Itoh T, and Fujiwara R (2013) Expression pattern of human ATP-binding cassette transporters in skin. *Pharmacol Res Perspect* **1**:e00005.
- Toomvliet R, van Berckel BN, Luurtsema G, Lubberink M, Geldof AA, Bosch TM, Oerlemans R, Lammertsma AA, and Franssen EJ (2006) Effect of age on functional P-glycoprotein in the blood-brain barrier measured by use of (R)-[(11)C]verapamil and positron emission tomography. *Clin Pharmacol Ther* **79**:540–548.
- Worm J, Kirkin AF, Dzhandzhugazyan KN, and Gulberg P (2001) Methylation-dependent silencing of the reduced folate carrier gene in inherently methotrexate-resistant human breast cancer cells. *J Biol Chem* **276**:39990–40000.
- Wu LX, Wen CJ, Li Y, Zhang X, Shao YY, Yang Z, and Zhou HH (2015) Interindividual epigenetic variation in ABCB1 promoter and its relationship with ABCB1 expression and function in healthy Chinese subjects. *Br J Clin Pharmacol* **80**:1109–1121.
- Yang BT, Dayeh TA, Volkov PA, Kirkpatrick CL, Malmgren S, Jing X, Renström E, Wollheim CB, Nitert MD, and Ling C (2012) Increased DNA methylation and decreased expression of PDX-1 in pancreatic islets from patients with type 2 diabetes. *Mol Endocrinol* **26**:1203–1212.
- Yasar U, Greenblatt DJ, Guillemette C, and Court MH (2013) Evidence for regulation of UDP-glucuronosyltransferase (UGT) 1A1 protein expression and activity via DNA methylation in healthy human livers. *J Pharm Pharmacol* **65**:874–883.
- Yoon B, Herman H, Hu B, Park YJ, Lindroth A, Bell A, West AG, Chang Y, Stablewski A, Piel JC, et al. (2005) Rasgrf1 imprinting is regulated by a CTCF-dependent methylation-sensitive enhancer blocker. *Mol Cell Biol* **25**:11184–11190.
- Yoon BJ, Herman H, Sikora A, Smith LT, Plass C, and Soloway PD (2002) Regulation of DNA methylation of Rasgrf1. *Nat Genet* **30**:92–96.
- Young LC, Campling BG, Cole SP, Deeley RG, and Gerlach JH (2001) Multidrug resistance proteins MRP3, MRP1, and MRP2 in lung cancer: correlation of protein levels with drug response and messenger RNA levels. *Clin Cancer Res* **7**:1798–1804.
- Young LC, Campling BG, Voskoglou-Nomikos T, Cole SP, Deeley RG, and Gerlach JH (1999) Expression of multidrug resistance protein-related genes in lung cancer: correlation with drug response. *Clin Cancer Res* **5**:673–680.
- Zolk O, Schnepf R, Muschler M, Fromm MF, Wendler O, Traxdorf M, Iro H, and Zenk J (2013) Transporter gene expression in human head and neck squamous cell carcinoma and associated epigenetic regulatory mechanisms. *Am J Pathol* **182**:234–243.

Address correspondence to: Ichiro Ieiri, Department of Clinical Pharmacokinetics, Graduate School of Pharmaceutical Sciences, Kyushu University, 3-1-1 Maidashi, Higashi-ku, Fukuoka 812-8582, Japan. E-mail: ieiri-tr@umin.ac.jp